

LATE REIONIZATION BY SUPERNOVA DRIVEN WINDS¹

Max Tegmark¹, Joseph Silk² & August Evrard³

¹*Department of Physics, University of California, Berkeley, California 94720*

²*Departments of Astronomy and Physics, and Center for Particle Astrophysics,
University of California, Berkeley, California 94720*

³*Department of Physics, University of Michigan, Ann Arbor, Michigan 48109*

Abstract

A model is presented in which supernova-driven winds from early galaxies reionize the intergalactic medium by $z = 5$. This scenario can explain the observed absence of a Gunn-Peterson trough in the spectra of high-redshift quasars providing that the bulk of these early galaxies are quite small, no more massive than about $10^8 M_\odot$. It also predicts that most of the IGM was enriched to at least 10% of current metal content by $z = 5$ and perhaps as early as $z = 15$. The existence of such early mini-galaxies violates no spectral constraints and is consistent with a pure CDM model with $b \leq 2$. Since the final radius of a typical ionized bubble is only around 100 kpc, the induced modification of the galaxy autocorrelation function is negligible, as is the induced angular smoothing of the CBR. Some of the gas swept up by shells may be observable as pressure-supported Lyman-alpha forest clouds.

¹ Published in *ApJ*, **417**, 54, November 1, 1993.

Submitted September 9 1992, accepted March 24. Available from
<http://www.sns.ias.edu/~max/gp.html> (faster from the US) and from
<http://www.mpa-garching.mpg.de/~max/gp.html> (faster from Europe).

1 Introduction

The absence of a Gunn-Peterson trough in the spectra of high-redshift quasars has provided strong evidence for the intergalactic medium (IGM) being highly ionized as early as $z = 4$ (Gunn & Peterson 1965; Steidel and Sargent 1987; Webb *et al.* 1992). The hypothesis that photoionization of the IGM by quasars could account for this ionization (Arons & McCray 1969; Bergeron & Salpeter 1970; Sherman 1980) has been challenged (Shapiro 1986; Shapiro & Giroux 1987; Miralda-Escude & Ostriker 1990). Other studies have maintained that photoionization by quasars (Donahue & Shull 1987) or active galactic nuclei (Terasawa 1992) may nonetheless be sufficient. However, in view of the large uncertainties in crucial parameters such as ionizing fluxes, the issue of what reionized the IGM must still be considered open.

In comparing the Gunn-Peterson constraints with our work in papers 3 and 4, the crucial difference is the degree of ionization required. To affect the CBR, it does not really matter whether the ionization fraction x is 90% or 99.999%, as this makes only a 10% difference in the optical depth τ . The Gunn-Peterson limits constrain not x but $(1 - x)$, the neutral fraction. Thus in this context, the difference between 90% and 99.999% ionization is four orders of magnitude. In papers 3 and 4, we found that photoionization by early galaxies could easily reionize the IGM by a redshift $z = 5$, but the issue here is whether photoionization alone can provide the extremely high ionization fraction required to pass the Gunn- Peterson test.

In this paper, we investigate an alternative reionization scenario, which produces considerably higher IGM temperatures than those attained by the photoionization models in previous papers. Supernova driven winds from luminous galaxies have long been conjectured to be an important ionization source for the IGM (Schwartz *et al.* 1975; Ikeuchi & Ostriker 1986; Carlberg & Couchman 1989). Cold dark matter (CDM)-based models of structure formation (Blumenthal *et al.* 1984; Efstathiou *et al.* 1985) predict the formation of gravitationally bound objects of mass as small as $10^7 M_\odot$ in large numbers before $z = 5$. Recent work (Blanchard *et al.* 1992) indicates that such objects can cool rapidly and presumably fragment into stars. These early mini-galaxies would be expected to release great amounts of kinetic energy into the surrounding IGM, thereby creating large, fairly spherical voids filled with thin, hot, ionized plasma. We analyze the effect of expanding bubbles driven by supernova winds from early mini-galaxies, and show that this mechanism of distributing energy can indeed provide the required

ionization without violating any of the current spectral constraints.

In Section 2, we will treat the expansion of a shell in a uniform, cold and neutral IGM. As these bubbles become larger and more numerous and fill most of space, this obviously becomes a very poor model of the IGM. In Section 3 we estimate bulk properties of this new processed IGM such as temperature, density and ionization.

2 The Explosion Model

Since the pioneering work on spherically symmetric explosions by Sedov (1959), a profusion of analytic solutions have been given by numerous authors for models of ever-increasing complexity (Cox & Smith 1974; McKee & Ostriker 1977; Weaver *et al.* 1977; McCray & Snow 1979; Bruhweiler *et al.* 1980; Tomisaka *et al.* 1980; McCray & Kafatos 1987; Ostriker & McKee 1988). Most of these models pertain to bubbles in the interstellar medium of a galaxy, where the expansion of the universe can be ignored. Ostriker & McKee have given asymptotic self-similarity solutions that incorporate this latter complication, but unfortunately they are not sufficiently accurate for our needs. The reason is that since neither energy nor momentum is conserved in the regime before the shell becomes self-similar, there is no accurate way to normalize the self-similar solution using the initial data.

Let ρ_b and ρ_d denote the average densities of baryonic and non-baryonic matter in the universe. We will assume that all baryons are in diffuse form early on, so that ρ_b is also the density of the IGM. We will write $\rho_b = \Omega_b \rho_c$ and $\rho_d = \Omega_d \rho_c$, where the critical density $\rho_c \equiv 3H^2/8\pi G$. We will use a three-phase model for the expanding bubbles:

- a dense, fairly cool spherical shell of outer radius R and thickness $R\delta$, containing a fraction $(1 - f_m)$ of the total baryonic mass enclosed,
- uniform neutral ambient intergalactic medium (IGM) of density $\rho_b + \rho_d$ and zero pressure outside,
- a hot, thin, isothermal plasma of pressure p and temperature T inside the shell.

The shell is driven outwards by the pressure of the hot interior plasma but slowed by the IGM and by gravity. The plasma is heated by kinetic energy from supernova explosions and collisions with IGM and cooled by bremsstrahlung and Compton drag against the cosmic background radiation.

2.1 The expanding shell

We assume that the expanding shell sweeps up almost all baryonic IGM that it encounters and loses only a small fraction of it through evaporation into the interior, so that its total mass is given by $m(t) = \frac{4}{3}\pi R(t)^3(1 - f_m)\rho_b$, where the constant $f_m \ll 1$. Since $\dot{\rho}_b/\rho_b = -3H$ for any cosmological model, we get

$$\frac{\dot{m}}{m} = \left(R^3\rho_b\right)^{-1} \frac{d}{dt} \left(R^3\rho_b\right) = 3 \left(\frac{\dot{R}}{R} - H\right) \text{ if } \frac{\dot{R}}{R} > H, \text{ zero otherwise.}$$

(The shell will acquire new mass when it is expanding faster than the Hubble flow, and will never lose mass.) It turns out that the Hubble flow catches up with the shell only as $t \rightarrow \infty$, so we will always have $\dot{R} > HR$ and $\dot{m} > 0$.

When new mass is swept up, it must be accelerated from the velocity HR to \dot{R} , so the shell experiences a net braking force $(\dot{R} - HR)\dot{m}$. The interior pressure p drives the shell outward with a force $pA = 4\pi R^2 p = 3mp/\rho_b R$ in the thin shell approximation $\delta, f_m \ll 1$. Finally there is a gravitational braking force, which in the thin-shell approximation (Ostriker & McKee 1988) gives the deceleration $\frac{4}{3}\pi GR(\rho_d + \frac{1}{2}\rho_b)$. Adding these three force terms, the radial equation of motion becomes

$$\ddot{R} = \frac{8\pi pG}{\Omega_b H^2 R} - \frac{3}{R} (\dot{R} - HR)^2 - \left(\Omega_d + \frac{1}{2}\Omega_b\right) \frac{H^2 R}{2}. \quad (1)$$

2.2 The interior plasma

The equation of state for the plasma in the hot interior gives the thermal energy

$$E_t = \frac{3}{2}pV = 2\pi pR^3, \quad (2)$$

and energy conservation for the interior yields

$$\dot{E}_t = L - pdV/dt = L - 4\pi pR^2\dot{R}, \quad (3)$$

where the luminosity L incorporates all sources of heating and cooling of the plasma. We will consider five contributions to L and write

$$L = L_{sn} - L_{comp} - L_{brems} - L_{ion} + L_{diss},$$

where L_{sn} is the energy injection from supernova explosions, L_{comp} the cooling by Compton drag against the CBR, L_{brems} the cooling by bremsstrahlung,

L_{ion} the cooling by ionization of neutral IGM and L_{diss} the heating from collisions between the shell and the IGM.

In stellar burning from zero to solar metallicity, the mass fraction 0.02×0.007 is released, mostly as radiation. Due to low cross-sections, only a negligible fraction of this radiation will contribute towards heating the gas, so we will only be interested in the energy that is released in kinetic form. From empirical observations of active galactic winds (Heckman 1990) about 2% of the total luminosity from a galaxy is mechanical. Another empirical observation is that for a solar neighborhood initial stellar mass function, one has roughly one supernova for every $150M_{\odot}$ of baryons that form stars, with a typical kinetic energy output of 10^{51} ergs per explosion. Both of these observations lead to the same estimate

$$L_{sn} = \frac{f_{sn}M_b c^2}{t_{burn}} \theta(t_{burn} - t) \approx 1.2L_{\odot} \frac{M_b}{M_{\odot}} \theta(t_{burn} - t),$$

where the efficiency $f_{sn} \approx 4 \times 10^{-6}$ and where we have assumed that the energy is released at a constant rate during a period $t_{burn} \approx 5 \times 10^7$ years.

Now let us examine cooling. The interior baryon density is $\rho_i = \rho_b f_m / (1 - \delta)^3$ whereas the shell density is $\rho_s = \rho_b (1 - f_m) / (1 - (1 - \delta)^3) \approx \rho_b / 3\delta$ if $f_m, \delta \ll 1$. Compton drag against the microwave background radiation causes energy loss at a rate (Kompaneets 1957)

$$L_{comp} = \frac{4\pi^2}{15} (\sigma_t c n_e) \left(\frac{kT_e}{m_e c^2} \right) \left(\frac{kT_{\gamma}}{\hbar c} \right)^4 \hbar c V, \quad (4)$$

where σ_t is the Thomson cross section, $V = \frac{4}{3}\pi R^3$, and $T_e = T$, the temperature of the interior plasma, which is given by

$$E_t = \left(\frac{3}{2} + \frac{3}{2} \right) kT \frac{f_m \rho_b}{m_p} V.$$

(We will assume almost complete ionization and low metallicity, so that $n_e \approx f_m n_b$.) Using equation (2), we see that Compton drag causes cooling on a timescale

$$\frac{E_t}{L_{comp}} = \frac{45}{4\pi^2} \left(\frac{\hbar c}{kT_{\gamma}} \right)^4 \frac{m_e}{\sigma_t \hbar} \approx 2 \times 10^{12} \text{ years} \times (1+z)^{-4},$$

that is, it becomes important only at high redshifts. It turns out that $L_{brems} \ll L_{comp}$ in our regime of interest, so we will simply make the approximation $L_{brems} \approx 0$. Assuming that the ambient IGM is completely

neutral, the power required to ionize the hydrogen entering the interior is simply

$$L_{ion} = f_m n_b E_0 \times 4\pi R^2 [\dot{R} - HR],$$

where $E_0 \approx 13.6 \text{ eV}$.

The equation of motion (1) assumes that the collisions between the expanding shell and the ambient IGM are perfectly inelastic. The kinetic energy dissipated has one of three fates: It may

- (a) radiate away in shock cooling processes,
- (b) ionize the swept up IGM, or
- (c) heat the shell and by conduction heat the interior plasma.

Let f_d denote the fraction that is reinjected into the interior plasma through processes (b) and (c). This is one of the major uncertainties of the model. Now a straightforward kinematic calculation of the kinetic energy loss per unit time gives

$$L_{diss} = f_d \frac{3m}{2R} (\dot{R} - HR)^3.$$

Making accurate estimates of f_d is difficult, so we simply use the two extreme cases $f_d = 0$ and $f_d = 1$ in the simulations. Perhaps surprisingly, the results will be seen to be relatively independent of the choice of f_d .

2.3 Solutions to the equations

Combining (2) and (3) leaves us with

$$\dot{p} = \frac{L}{2\pi R^3} - 5\frac{\dot{R}}{R}p. \quad (5)$$

The system of equations (1) and (5) reduces to that derived by Weaver *et al.* (1977) in the special case where $L(t)$ is constant and the expansion of the universe is ignored.

Let us define dimensionless variables as follows:

$$\begin{aligned} \tau &\equiv t/t_*, & t_* &\equiv \frac{2}{3}H_0^{-1}(1+z_*)^{-3/2} \\ \eta &\equiv H/H_*, & H_* &\equiv \frac{2}{3}t_*^{-1} \\ \ell &\equiv L/L_*, & L_* &\equiv f_{sn}M_b c^2 t_{burn}^{-1} \approx 1.2 \times 10^5 L_\odot \times M_5 \end{aligned}$$

$$\begin{aligned}
\varepsilon &\equiv E/E_*, & E_* &\equiv L_* t_{burn} && \approx 7.2 \times 10^{53} \text{ ergs} \times M_5 \\
r &\equiv R/R_*, & R_* &\equiv L_*^{1/5} G^{1/5} t_* && \approx 0.13 \text{ Mpc} \times h^{-1} (1+z_*)^{-3/2} M_5^{1/5} \\
q &\equiv p/p_*, & p_* &\equiv L_*^{2/5} G^{-3/5} t_*^{-2} && \approx 1.4 \times 10^{-16} \text{ Pa} \times h^2 (1+z_*)^3 M_5^{2/5}
\end{aligned}$$

Here we have taken $h = 0.5$ and defined $M_5 \equiv M_b/10^5 M_\odot$. If $\Omega \equiv \Omega_b + \Omega_d=1$, then t_* is the age of the universe at the redshift z_* when the shell begins its expansion, i.e. the Big Bang occurred at $\tau = -1$ and the shell starts expanding at $\tau = 0$. For this simple case, we have $\eta = (1 + \tau)^{-1} = (1 + z_*)^{-3/2} (1 + z)^{3/2}$.

Equations (1) and (5) now become

$$\begin{cases} r''(\tau) = \frac{18\pi}{\Omega_b} \eta(\tau)^{-2} \frac{q(\tau)}{r(\tau)} - 3 \left(1 - \frac{2}{3} \frac{\eta(\tau)r(\tau)}{r'(\tau)}\right)^2 \frac{r'(\tau)^2}{r(\tau)} - \left(\frac{2}{9}\Omega_d + \frac{1}{9}\Omega_b\right) \eta(\tau)^2 r(\tau) \\ q'(\tau) = \frac{\ell(\tau)}{2\pi r(\tau)^3} - 5 \frac{r'(\tau)}{r(\tau)} q(\tau) \end{cases} \quad (6)$$

Here $\ell = \ell_{sn} - \ell_{comp} - \ell_{ion} + \ell_{diss}$, where

$$\begin{aligned}
\ell_{sn} &= \theta(t_{burn} - t_*\tau), \\
\ell_{comp} &\approx 0.017h^{-1}(1+z_*)^{-3/2}(1+z)^4 r^3 q, \\
\ell_{ion} &\approx 2.2f_m \Omega_b M_5^{-2/5} \times \eta^2 r^2 \left(r' - \frac{2}{3}\eta r\right), \text{ and} \\
\ell_{diss} &= \frac{1}{3}f_d \Omega_b \times (\eta r)^2 \left(r' - \frac{2}{3}\eta r\right)^3.
\end{aligned}$$

In computing ℓ_{comp} , we have taken $T_{\gamma 0} = 2.74K$. The interior temperature, the thermal energy and the kinetic energy are given by

$$\begin{aligned}
T &\approx 4.5 \times 10^5 K \times \frac{M_5^{2/5} q(\tau)}{f_m \Omega_b \eta(\tau)^2}, \\
\varepsilon_t &= \frac{2\pi}{\tau_{burn}} r^3 q, \\
\varepsilon_k &= \frac{m\dot{R}^2/2}{L_* t_{burn}} = \frac{\Omega_b}{9\tau_{burn}} \eta^2 r^3 r'^2.
\end{aligned}$$

The solution to the system (6) evolves through three qualitatively different regimes: $\tau \ll 1$, $\tau \approx 1$ and $\tau \gg 1$.

a) In the limit of small times $\tau \ll 1$, gravity and Hubble flow are negligible and we obtain the asymptotic power law solution

$$r(\tau) = a\tau^{3/5}, \quad q(\tau) = b\tau^{-4/5}$$

$$\text{where } a \equiv \left(\frac{375/\Omega_b}{77 - 27f_d} \right)^{1/5} \quad \text{and} \quad b \equiv \frac{7\Omega_b}{150\pi} a^2, \quad (7)$$

as may be verified by direct substitution. This solution reduces to that found by Weaver *et al.* in the special case $f_d = 0$. Since the total energy injected is simply $\varepsilon_{in} = \tau/\tau_{burn}$, this gives

$$\frac{\varepsilon_t}{\varepsilon_{in}} = \frac{35}{77 - 27f_d} \quad \text{and} \quad \frac{\varepsilon_k}{\varepsilon_{in}} = \frac{15}{77 - 27f_d}$$

for small τ . Hence even though $\varepsilon_t + \varepsilon_k = \varepsilon_{in}$ only for the most optimistic case $f_d = 1$, we see that no more than $1 - \frac{35+15}{77} \approx 25\%$ of the injected energy is lost as radiation even in the worst case $f_d = 0$.

b) The behavior in the intermediate regime is a complicated interplay between several different effects:

1. After approximately 5×10^7 years, the supernova explosions cease, which slows the expansion. In this pressure-driven snowplow phase, we would asymptotically have $R \propto t^{2/7}, t^{4/13}, t^{1/3}, t^{4/11}$ or $t^{2/5}$ if there were no gravity, no Hubble flow and no cooling with $f_d = 0, \frac{1}{8}, \frac{1}{3}, \frac{5}{8}$ or 1, respectively.
2. Cooling (and pdV) work reduces the pressure and the thermal energy to virtually zero, which slows the expansion. With zero pressure, we would approach the momentum-conserving snowplow solution $R \propto t^{1/4}$ if there were no gravity and no Hubble flow.
3. The density of the IGM drops and the IGM already has an outward Hubble velocity before it gets swept up, which boosts the expansion and adds kinetic energy to the shell.
4. Gravity slows the expansion.
5. Dark matter that has been accelerated outward by the shell catches up with it again and speeds up the expansion. (This last effect has been neglected in the equations above, since it generally happens too late to be of importance for our purposes.)

c) As $t \rightarrow \infty$, the shell gets frozen into the Hubble flow, *i.e.* $R \propto t^{2/3}$ if $\Omega = 1$. An approximate analytic solution for $\tau \gg 1$ is given by Ostriker & McKee (1988), but since neither energy nor momentum is conserved in the intermediate regime, there is no simple way to connect this solution with the short-time solution above.

Numerical solutions for the comoving radius $(1+z)R$ are plotted in Figure 1 for different values of z_* and f_d . The asymptotic solution (7) has been used to generate initial data at $\tau = 0.01$ for the numerical integration. In this Figure, we have truncated R when the interior temperature drops below 15,000K, after which newly swept up IGM fails to become ionized. Figures 2, 3 and 4 show what becomes of the injected energy for different parameter values. Note that the relative fractions are approximately constant early on, while the supernovae inject energy, in accordance with the asymptotic solution (7). The reason that the total energy exceeds 100% of the input is that the shell gobbles up kinetic energy from swept-up IGM that already has an outward Hubble velocity.

3 Cosmological Consequences

Once the expanding bubbles discussed in the previous section have penetrated most of space, the IGM will presumably have a frothy character on scales of a few 100 kpc, containing thick and fairly cool shell fragments separated by large, hot, thin and ionized regions that used to be bubble interiors.

In Section 3.1, we calculate at what point the IGM becomes frothy, more specifically what fraction of space is covered by expanding shells at each z . In 3.2 we discuss the resulting enrichment of the IGM with heavy elements. In 3.3 the thermal history of the IGM after this epoch is treated. Finally, in 3.4 the residual ionization is computed, given this thermal history, and we discuss the circumstances under which the Gunn-Peterson constraint is satisfied.

3.1 IGM porosity

Assuming the standard PS theory of structure formation (Press & Schechter 1974), the fraction of all mass that has formed gravitationally bound objects of total (baryonic and non-baryonic) mass greater than M at redshift z is

$$1 - \operatorname{erf} \left[\frac{\delta_c}{\sqrt{2}\sigma(M)} \right],$$

where $\operatorname{erf}(x) \equiv 2\pi^{-1/2} \int_0^x e^{-u^2} du$ and σ^2 is the linearly extrapolated r.m.s. mass fluctuation in a sphere of radius r_0 . The latter is given by top-hat

filtering of the power spectrum as

$$\sigma^2 \equiv \left(\frac{\sigma_0}{1+z} \right)^2 \propto \frac{1}{(1+z)^2} \int_0^\infty \left[\frac{\sin kr_0}{(kr_0)^3} - \frac{\cos kr_0}{(kr_0)^2} \right]^2 P(k) dk, \quad (8)$$

where r_0 is given by $\frac{4}{3}\pi r_0^3 \rho = M$ and where $P(k)$ is the power spectrum. Although this approach has been criticized as too simplistic, numerical simulations (Efstathiou *et al.* 1988; Efstathiou & Rees 1988; Carlberg & Couchman 1989) have shown that it describes the mass distribution of newly formed structures remarkably well. Making the standard assumption of a Gaussian density field, Blanchard *et al.* (1992) have argued that it is an accurate description at least in the low mass limit. Since we are interested only in extremely low masses such as $10^6 M_\odot$, it appears to suffice for our purposes.

We choose $\delta_c = 1.69$, which is the linearly extrapolated overdensity at which a spherically symmetric perturbation has collapsed into a virialized object (Gott & Rees 1975). Letting f_g denote the fraction of all baryons in galaxies of mass greater than M at z , this would imply that

$$f_g \approx 1 - \operatorname{erf} \left[\frac{1.69(1+z)}{\sqrt{2}\sigma_0(M)} \right] \quad (9)$$

if no other forces than gravity were at work. However, it is commonly believed that galaxies correspond only to such objects that are able to cool (and fragment into stars) in a dynamical time or a Hubble time (Binney 1977; Rees & Ostriker 1977; Silk 1977; White & Rees 1978). Hence the above value of f_g should be interpreted only as an upper limit.

A common assumption is that the first galaxies to form have a total (baryonic and dark) mass $M_c \approx 10^6 M_\odot$, roughly the Jeans mass at recombination. Blanchard *et al.* (1992) examine the interplay between cooling and gravitational collapse in considerable detail, and conclude that the first galaxies to form have masses in the range $10^7 M_\odot$ to $10^8 M_\odot$, their redshift distribution still being given by equation (9). To keep things simple we will assume that all early galaxies have the same mass M_c and compare the results for $M_c = 2 \times 10^6 M_\odot$, $10^8 M_\odot$ and $10^{11} M_\odot$.

Let $R(z; z_*)$ denote the radius of a shell at z that was created at z_* by a galaxy of baryonic mass $M_b = \Omega_b M_c$ as in Section 2. Then the *naive filling factor*, the total bubble volume per unit volume of the universe, is

$$\phi(z) = \int_z^\infty \frac{4}{3}\pi R(z; z_*)^3 \frac{\rho_b}{M_b} \frac{df_g(z_*)}{d(-z_*)} dz_* = \phi_*(1+z)^3 \int_z^\infty \frac{r(z; z_*)^3}{(1+z_*)^{9/2}} \frac{df_g(z_*)}{d(-z_*)} dz_*, \quad (10)$$

where

$$\phi_* \approx 1600h^{-1}M_5^{-2/5}(\Omega_b/0.06).$$

Clearly nothing prohibits ϕ from exceeding unity. This means that nearby shells have encountered each other and that certain volumes are being counted more than once. If the locations of the bubbles are uncorrelated, then the fraction of the universe that will be in a bubble, the *porosity*, is given by

$$P \equiv 1 - e^{-\phi}.$$

If the early galaxies are clustered rather than Poisson-distributed, this value is an overestimate. For an extreme (and very unrealistic) example, if they would always come in clusters of size n and the clusters would be much smaller than the typical bubble size of 100 kpc, then it is easy to see that $P \approx 1 - e^{-\phi/n}$. For more realistic cases, simple analytic expressions for P are generally out of reach. Since we expect the clustering to be quite weak, we will use the Poisson assumption for simplicity.

The uppermost panels of Figures 5 and 6 contain $P(z)$ for various parameter values, calculated numerically from equation (10) using the numerical solutions for $r(z; z_*)$. It is seen that the lower mass in Figure 5 ($2 \times 10^6 M_\odot$ versus $10^8 M_\odot$) gives higher filling factors, so that the expanding shells fill almost 100% of space by $z = 5$ for three of the four choices of $f_g(5)$. In 6, we see that almost 20% of the baryons must be in galaxies by $z = 5$ to achieve this. The greater efficiency of small galaxies is to be expected, since $\phi_* \propto M^{-2/5}$. Although some parameters still yield the desired $P \approx 100\%$ by $z = 5$ in Figure 6, using present-day masses like $M_c = 10^{11} M_\odot$ fails dismally (not plotted) for all choices of the other parameters. Roughly, the largest M_c that works is $10^8 M_\odot$.

As can be seen, the dependence on f_d (dashed versus solid lines) is rather weak.

In order to calculate $\sigma_0(M_c)$ from the fluctuations observed on larger scales today, we need detailed knowledge of the power spectrum down to very small scales, something which is fraught with considerable uncertainty. For this reason, we have chosen to label the curves by the more physical parameter $f_g(5)$, the fraction of all baryons that have formed galaxies by $z = 5$. The four sets of curves correspond to fractions of 50%, 20%, 10% and 1%. These percentages should be compared with observational estimates of metallicity, as will be discussed in Section 3.2.

The second column of Table 1 contains the values $\sigma_0(M_c)$ necessary to obtain various values of $f_g(5)$, calculated by inverting the error function

$f_g(5)$	$\sigma_0(M_c)$	$b_{cdm,6}$	$b_{cdm,8}$	$b_{tilted,6}$	$b_{tilted,8}$
1%	3.94	4.8	3.5	2.5	2.0
10%	6.18	3.1	2.2	1.6	1.3
20%	7.92	2.4	1.7	1.2	1.0
50%	15.06	1.3	0.9	0.6	0.5

Table 1: Correspondence between various ways of normalizing the power spectrum

in equation (9). The last four columns contain the bias factors necessary to yield this value of $\sigma_0(M_c)$ for two choices of power spectra (CDM and $n=0.7$ tilted CDM) and two choices of cutoff mass ($M_c = 2 \times 10^6 M_\odot$ and $M_c = 10^8 M_\odot$). Thus $b = \gamma/\sigma_0(M_c)$, where we define γ to be the ratio between σ at M_c and σ at $8h^{-1} \text{Mpc} \equiv b^{-1}$. Performing the integral (8) numerically with the CDM transfer function given by Bardeen *et al.* 1986 (BBKS), $h = 0.5$, $\Omega = 1$, $\Omega_b \ll 1$ and an $n = 1$ Harrison-Zel'dovich initial spectrum gives $\gamma \approx 19.0$ for $M_c = 2 \times 10^6 M_\odot$ and $\gamma \approx 13.6$ for $M_c = 10^8 M_\odot$. Using the CDM transfer function of Bond and Efstathiou (1984) instead gives $\gamma \approx 18.1$ and $\gamma \approx 13.7$, respectively. The BBKS transfer function is more applicable here since it includes the logarithmic dependence that becomes important for very low masses. The BBKS transfer function with a tilted ($n=0.7$) primordial spectrum yields the significantly lower values $\gamma \approx 9.71$ and $\gamma \approx 7.93$, respectively.

Basically, Table 1 shows that any of our values of $f_g(5)$ become consistent with a feasible bias factor for some choice of power spectrum and cutoff mass.

3.2 IGM enrichment

These values of $f_g(5)$ should be compared with observational estimates of metallicity, since if the stars in these early mini-galaxies produce the same fractions of heavy elements as do conventional stars, then these percentages are directly linked to the fraction of currently observed metals that were made before $z = 5$. Some of the enriched shells may be observable as quasar absorption line systems, as intracluster gas, and, indirectly, as in the metallicities of old disk and halo stars.

Observations of iron abundances in intracluster gas by HEAO-1, Exosat and Ginga (*e.g.* Mushotzky 1984; Hughes *et al.* 1988; Edge 1989; Hatsukade

1989) have shown that most clusters have abundances between 25% and 50% of the solar value. Einstein observations have showed the presence of a large variety of other heavy elements in the intracluster gas (Lea *et al.* 1982; Rothenflug *et al.* 1984). Most of this gas and some of these metals are believed to be “primordial”, since the gas mass in clusters is typically several times greater than the observed stellar mass in the cluster galaxies (Blumenthal *et al.* 1984; David *et al.* 1990; Arnaud *et al.* 1991).

There are indications that the most of these heavy elements may have been produced as recently as around $z = 2-3$, and that the metallicity in the halo gas of some $z \approx 3$ galaxies inferred from QSO absorption line studies are as low as 0.1% of the solar value (Steidel 1990). However, this and other observations of extremely metal-poor objects (Pettini *et al.* 1990) does not necessarily rule out our scenario, since it is highly uncertain whether all the hydrogen in the swept-up IGM would get thoroughly mixed with the metal-rich supernova ejecta.

3.3 IGM temperature

Let $T(z; z_*)$ denote the temperature of the interior of a bubble at z that was created at z_* as in Section 2. Then the volume-averaged temperature of the IGM is

$$\begin{aligned}
 T_{IGM}(z) &\equiv \int_z^\infty \frac{4}{3} \pi R(z; z_*)^3 T(z; z_*) \frac{\rho_b}{M_b} \frac{df_g(z_*)}{d(-z_*)} dz_* \\
 &= \phi_*(1+z)^3 \int_z^\infty \frac{r(z; z_*)^3}{(1+z_*)^{9/2}} T(z; z_*) \frac{df_g(z_*)}{d(-z_*)} dz_*. \quad (11)
 \end{aligned}$$

When ϕ becomes of order unity, the IGM swept up by the expanding shells is no longer cold, neutral and homogeneous, so the treatment in Section 2 breaks down. The resulting temperatures will be underestimated, since less thermal energy needs to be expended on heating and ionization. As can be seen in Figures 5 and 6, the transition from $\phi \ll 1$, where the treatment in Section 2 is valid, to $\phi \gg 1$, where the IGM becomes fairly uniform, is quite rapid. Since T_{IGM} defined above is proportional to the thermal energy per unit volume, energy conservation leads us to assume that T_{IGM} remains fairly constant during this transition and therefore is a good estimate of the bulk IGM temperature immediately afterwards. From this time on, we will approximate the IGM outside the scattered dense and cold shell remnants by a uniform isothermal plasma. Applying equations (2), (3) and (4) to the

IGM yields the following equation for its thermal evolution:

$$-\frac{d}{dz}T_5 = -\left[\frac{2}{1+z} + A(1+z)^{3/2}\right]T_5 + \ell_{inj}, \quad (12)$$

where the first term encompasses cooling from adiabatic expansion and the second term Compton cooling. $T_5 \equiv T_{IGM}/10^5 K$, $A \equiv 1.5(t_0/t_{comp}) \approx 0.0042h^{-1}$ and $\ell_{inj} \equiv t_0 L_{inj}/k \times 10^5 K$, where L_{inj} is the power injected into the IGM per proton from all heat sources combined. The Compton cooling term is seen to increase with redshift, equaling the adiabatic term at $z \approx 17h^{0.4} - 1$.

In the most pessimistic case of no reheating whatsoever, *i.e.* for $\ell_{inj} = 0$, equation (12) has the solution

$$T \propto (1+z)^2 e^{0.4A(1+z)^{5/2}}.$$

A more optimistic assumption is that some fraction f_{inj} of the total energy released from stellar burning in newly formed galaxies continues to heat the IGM, *i.e.*

$$\ell_{inj} = f_{inj} \left(\frac{0.02 \times 0.007 m_p c^2}{k \times 10^5 K} \right) \frac{df_g}{d(-z)} \approx \left(\frac{2.1 \times 10^4}{\sigma_0} \right) f_{inj} \exp \left(-\frac{1}{2} \left[\frac{1.69(1+z)}{\sigma_0(M_c)} \right]^2 \right),$$

which would also incorporate other modes of energy injection such as radiation. The middle panels in Figures 5 and 6 show the temperature resulting from $f_{inj} = 0, 0.001$ and 0.02 and different initial values. For $P < 0.8$, T_{IGM} has been calculated numerically from equation (11) by using the numerical solutions for $r(z; z_*)$. Then the value at the redshift for which $P = 0.8$ has been used as initial data for equation (12). For comparison, two horizontal lines have been added showing what temperatures would be required to obtain neutral fractions of 10^{-6} and 10^{-5} in *equilibrium*, using equation (13). Since the plasma is in fact out of equilibrium, these highly ionized states can be maintained at much lower temperatures, as is seen in the bottom plots.

3.4 IGM ionization and the Gunn-Peterson effect

Assuming that any neutral hydrogen in the remains of the shells will have insufficient time to diffuse far into the hot ionized regions that used to be shell interiors, we can treat the latter as an isolated mixture of gas and plasma where the ionization fraction χ evolves as

$$\dot{\chi} = n\chi [(1-\chi)\Lambda_{ion}(T) - \chi\Lambda_{rec}(T)],$$

and where the rates for collisional ionization and recombination are given by (Stebbins & Silk 1986)

$$\Lambda_{ion} = \langle \sigma_{ci} v \rangle \approx 7.2 a_0^2 \left(\frac{kT}{m_e} \right)^{1/2} e^{-E_0/kT},$$

$$\Lambda_{rec} = \langle \sigma_{rec} v \rangle \approx \frac{64\pi}{3\sqrt{3}\pi} \alpha^4 a_0^2 c \left(\frac{kT}{E_0} \right)^{-2/3},$$

where a_0 is the Bohr radius and α is the fine structure constant. Changing the independent variable to redshift, the $\Omega = 1$ case leaves us with

$$-\frac{d}{dz} \chi = \frac{3}{2} \frac{f_m \Omega_b}{(1-\delta)^3} (1+z)^{1/2} \chi [(1-\chi)\lambda_{ion}(\chi) - \chi\lambda_{rec}(T)],$$

$$\lambda_{ion}(T) \equiv n_{c0} t_0 \Lambda_{ion}(T) \approx [5.7 \times 10^4 h \Omega_b] T_5^{1/2} e^{1.58/T_5}$$

$$\lambda_{rec}(T) \equiv n_{c0} t_0 \Lambda_{rec}(T) \approx [0.16 h \Omega_b] T_5^{-2/3}.$$

For large enough z , the ionization fraction will adjust rapidly enough to remain in a quasistatic equilibrium and hence be given by $\dot{\chi} = 0$, *i.e.*

$$\chi = \left[1 + \frac{\Lambda_{rec}(T)}{\Lambda_{ion}(T)} \right]^{-1} \approx \left[1 + 2.8 \times 10^{-6} T_5^{-7/6} e^{1.58/T_5} \right]^{-1}. \quad (13)$$

The observed absence of a Gunn-Peterson trough in the spectra of high-redshift quasars strongly constrains the density of neutral hydrogen in the IGM. The most thorough study to date, involving eight quasars (Steidel & Sargent 1987), concluded that

$$\Omega_{H_I}(z = 2.64) < (1.2 \pm 3.1) \times 10^{-8} h_{50}^{-1}$$

if $\Omega = 1$. In our model this corresponds to $(1 - \chi) < (1.2 \pm 3.1) \times 10^{-8} / (f_m \Omega_b) \approx 2 \times 10^{-6}$ for $\Omega_b = 0.06$ and $f_m = 0.1$. Thus we are helped not only by the IGM being ionized, but also by it being diffuse. In a recent study of a single quasar, Webb *et al.* (1992) find the data consistent with either $\Omega_{H_I}(z = 4.1) = 0$ or $\Omega_{H_I}(z = 4.1) = 1.5 \times 10^{-8} h_{50}^{-1}$, depending on model assumptions. We will use the latter value as an upper limit. Finally, recent Hubble Space Telescope spectroscopy of 3C 273 has been used to infer that $\Omega_{H_I}(z = 0.158) < 1.4 \times 10^{-7} h_{50}^{-1}$. The constraints from these three studies are plotted in Figures 5 and 6 together with the ionization levels predicted by our scenario.

To achieve $\chi = 10^{-4}$, 10^{-5} and 10^{-6} in equilibrium would by equation (13) require $T > 5.5 \times 10^4 K$, $T > 1.1 \times 10^5 K$ and $T > 3.6 \times 10^5 K$, respectively. As can be seen from the numerical solutions in the bottom panels of Figures 5 and 6, the recombination rate is generally too slow for equilibrium to be established, and the IGM remains almost completely ionized even when $T \ll 15,000K$ and equilibrium would have yielded $\chi \approx 0$. In both 3a and 3b, a very moderate reheating ($f_{inj} = 0.001$, heavy lines) is seen to suffice to satisfy the three observational constraints. In the absence of any reheating whatsoever, the only models that satisfy the constraints are those with very low density ($\Omega_b = 0.01$ or $f_m = 0.01$).

In summary, the only parameters that are strongly constrained by the Gunn-Peterson test are M_c and $\sigma_0(M_c)$.

3.5 Other spectral constraints

Let us estimate to what extent Compton cooling of the hot plasma will distort the cosmic microwave background radiation (CBR). Since for $T_e \gg T_\gamma$ the Comptonization y-parameter (Stebbins & Silk 1986)

$$y_C \equiv \int_t^{t_0} \frac{kT_e}{m_e c^2} n_e \sigma_t c dt$$

is linear in the plasma energy density $\left(\frac{3}{2} + \frac{3}{2}\right) kT_e n_e$ at each fixed time ($T_e = T_{IGM}$), all that counts is the spatially averaged thermal energy density at each redshift. Since the former is simply $\varepsilon_t(z; z_*)$ times the density of injected energy $f_g f_{sn} \Omega_b \rho c^2$, the calculation reduces to mere energetics and we obtain

$$y_C = y_* \int_z^\infty \frac{df_g(z_*)}{d(-z_*)} \int_0^{z_*} \sqrt{1+z} \varepsilon_t(z; z_*) dz dz_*,$$

where

$$y_* \equiv \frac{1}{8} f_{sn} \Omega_b^2 \frac{\sigma_t c H}{m_p G} \approx 9 \times 10^{-7} h \Omega_b^2.$$

The current observational upper limit on y is 2.5×10^{-5} (Mather *et al.* 1994), so even if we take $f_g(0)$ as high as 100% and make a gross overestimate of the integral by making all our galaxies as early as at $z_* = 30$ and by replacing $\varepsilon_t(z; z_*)$ by its upper bound 60% for all z, z_* , our y is below the observational limit by three orders of magnitude for $\Omega = 1$.

Now let us estimate the optical depth of the IGM. It has long been known that reionization can cause a spatial smoothing of the microwave

background as CBR photons Thomson scatter off of free electrons. Since $n_e = \chi_{IGM} n_b$, the optical depth for Thomson scattering, i.e. the number of mean free paths that a CBR photon has traversed when it reaches our detectors, is

$$\tau_t = \int_{t_{rec}}^{t_0} \sigma_t \chi_{IGM} n_b c dt = \tau_t^* \int_0^{z_{rec}} \sqrt{1+z} \chi_{IGM} dz,$$

where

$$\tau_t^* \equiv \frac{3}{8\pi} f_m \Omega_b \frac{H_0 c \sigma_t}{m_p G} \approx 0.07 \Omega_b h.$$

Let us evaluate the integral by making the approximation that χ_{IGM} increases abruptly from 0 to 1 at some redshift z_{ion} . Then even for z_{ion} as high as 30, $\tau_t \approx 7.9 h \Omega_b f_m \approx 0.02 \ll 1$ for our fiducial parameter values $h = 0.5$, $\Omega_b = 0.06$ and $f_m = 0.1$, so the probability that a given CBR photon is never scattered at all is $e^{-0.02} \approx 98\%$. Hence this scenario for late reionization will have only a very marginal smoothing effect on the CBR. If the shells are totally ionized as well, then the factor f_m disappears from the expressions above which helps only slightly. Then $z_{ion} = 15$ would imply that 8% of the CBR would be spatially smoothed on scales of a few degrees.

4 Discussion

We have calculated the effects of supernova driven winds from early galaxies assuming a Press-Schechter model of galaxy formation and a CDM power spectrum. The calculations have shown that reionization by such winds can indeed explain the observed absence of a Gunn-Peterson effect if a number of conditions are satisfied:

1. The masses of the first generation of galaxies must be very small, not greater than about $10^8 M_\odot$.
2. There is enough power on these small scales to get at least 10% of the baryons in galaxies by $z = 5$.
3. Except for the case where Ω_b is as low as 0.01, there must be some reheating of the IGM after $z = 5$ to prevent the IGM from recombining beyond allowed levels.
4. The commonly used thin-shell approximation for expanding bubbles must remain valid over cosmological timescales, with the mass fraction in the interior remaining much less than unity.

Whether 1) is satisfied or not depends crucially on the model for structure formation. This scenario is consistent with a pure CDM model and some low-bias tilted CDM models, but not with top-down models like pure HDM.

Observations of nearly solar abundances of heavy elements in intracluster gas have given some support for 2), which is roughly equivalent to requiring that at least 10% of the heavy elements in the universe be made before $z = 5$ (or whenever $\phi \gg 1$). As discussed in Section 3.2, the observations of some extremely metal-poor objects in QSO absorption line studies do not necessarily rule out our scenario, since it is highly uncertain whether all the hydrogen in the swept-up IGM would get thoroughly mixed with the metal-rich supernova ejecta. The fact that large numbers of mini-galaxies are not seen today need not be a problem either. Possible explanations for this range from mechanisms for physically destroying them (Dekel & Silk 1986, for instance) to the fact that the faint end of the luminosity function is still so poorly known that old dwarf galaxies in the field may be too faint to see by the present epoch (Binggeli *et al.* 1988).

To violate 3), the actual reheating would have to be extremely small. A current IGM temperature between $10^4 K$ and $10^5 K$ suffices, depending on other parameter values, since the low density IGM never has time to reach its equilibrium ionization.

The thin-shell approximation 4) is obviously a weak point in the analysis, because of the simplistic treatment of the dense shell and its interface with the interior bubble. For instance, could the shell cool and fragment due to gravitational instability before it collides with other shells? An approximate analytic model for such instability has been provided by Ostriker & Cowie (1981). Their criterion is that instability sets in when $\Xi > 1$, where

$$\Xi \equiv \frac{2G\rho_{shell}R^2}{\dot{R}v_s}$$

and the sound speed $v_s = \sqrt{5kT/3m_p}$. In terms of our dimensionless variables, this becomes

$$\Xi \approx 0.011 \times M_5^{1/5} T_5^{-1/2} \left(\frac{\Omega_b}{0.06} \right) \left(\frac{\delta}{0.1} \right)^{-1} \left(\frac{1+z}{1+z_*} \right)^3 \frac{r^2}{r'}$$

which indicates that with our standard parameter values, gravitational instability does not pose problems even with fairly low shell temperatures.

The reason that the shell density is not limited to four times the ambient IGM density is that the jump condition is not adiabatic, due mainly to effective Compton cooling at the high redshifts under consideration.

After the critical z (typically between 20 and 5) at which the expanding shells have collided with neighbors and occupied most of space, the IGM is “frothy” on scales around 100 kpc, with dense cool shell remnants scattered in a hot thin and fairly uniform plasma. Since the dark matter distribution is left almost unaffected by the expanding bubbles, formation of larger structures such as the galaxies we observe today should remain fairly unaffected as far as concerns gravitational instability. There is indirect influence, however: the ubiquitous metals created by the early mini-galaxies would enhance the ability of the IGM to cool, which as mentioned in Section 3.1 is commonly believed to be crucial for galaxy formation.

Blanchard *et al.* (1992) argue that if the IGM has a temperature higher than the virial temperature of a dark halo, pressure support will prevent it from falling into the potential well and thus stop it from forming a luminous galaxy. The virial temperature they estimate for an object of mass M formed at a redshift z is approximately

$$T_{vir} \approx 5.7 \times 10^5 K \left(\frac{M}{10^{12} M_{\odot}} \right)^{2/3} (1+z)$$

for $h = 0.5$, so requiring $T_{vir} > T_{IGM}$ for say $T_{IGM} = 10^6 K$ at $z = 5$ would give a minimum galaxy mass of about $10^{11} M_{\odot}$. Such arguments indicate that the IGM reheating of our scenario might produce a “mass desert” between the earliest mini-galaxies and the galaxies we see today: The first generation of galaxies, mini-galaxies with masses of perhaps 10^6 or $10^8 M_{\odot}$, would keep forming until their expanding bubbles had occupied most of space and altered the bulk properties of the IGM. After that, formation of galaxies much smaller than those of today would be suppressed, since the IGM would be too hot. Eventually, as the IGM cools by adiabatic expansion, a progressively larger fraction of the IGM can be accreted by dark matter potential wells. Indeed, even with the volume averaged IGM temperature remaining hot due to some form of reheating, cooling flows in deep potential wells, in particular galaxy clusters, would not be suppressed. Late formation of galaxies is therefore possible.

Pressure balance between the shell and the interior during the expansion would give the ration $T_{shell}/T_{interior} = \rho_{b,interior}/\rho_{b,shell} \approx 3\delta f_m \approx 0.03$ for $\delta = f_m = 0.1$, so the shell fragments would expected to contain non-negligible fractions of neutral hydrogen and thus absorb some Lyman-alpha.

A typical shell radius is about 100 kpc for $M_c = 10^6 M_\odot$, a size comparable to that of the clouds of the Lyman-alpha forest. As to the number density of Lyman-alpha clouds, the observed velocity separations greatly exceed those we would expect if all shell fragments were to be identified with Lyman alpha clouds. Thus the majority of these fragments must have been destroyed by some other process. There are a number of ways in which this could occur, for instance through photoionization by UV flux from the parent galaxy or by collapse to form other dwarf galaxies. The resulting numbers resemble the abundance of minihalos in an alternative explanation of the Lyman-alpha forest (Rees 1986). Strong evolution, in the sense of an increasing cloud abundance with decreasing redshift, is expected to occur as cooling becomes effective.

The authors would like to thank Alain Blanchard for discussions on the subject of the paper and David Schlegel, Douglas Scott and Charles Steidel for many useful comments. This research has been supported in part by a grant from the NSF.

5 REFERENCES

- Arnaud, M., Rothenflug, R., Boulade, O., Vigroux, L. & Vangioni-Flam, E. 1992, *Astr. Ap.*, **254**, 49.
- Arons, J. & McCray, R. 1970, *Ap. Letters*, **5**, 123.
- Bardeen, J. M., Bond, J. R., Kaiser, N. & Szalay, A. S. 1986, *ApJ*, **304**, 15.
- Bergeron, J. & Salpeter, E. E. 1970, *Ap. Letters*, **7**, 115.
- Binney, J. 1977, *ApJ*, **215**, 483.
- Binggeli, B., Sandage, A. & Tammann, G. A. 1988, *Ann. Rev. Astr. Ap.*, **26**, 509.
- Blanchard, A., Valls-Gabaud, D. & Mamon, G. A. 1992, *Astr. Ap.*, **264**, 365.
- Blumenthal, G. R., Faber S. M., Primack, J. R., & Rees, M. J. 1984, *Nature*, **311**, 517.
- Bond, J. R. & Szalay, A. S. 1983, *ApJ*, **274**, 443.
- Bond, J. R. & Efstathiou, G. 1984, *ApJ (Letters)*, **285**, L45.
- Bruhweiler, F. C., Gull, T. R., Kafatos, M., & Sofia, S. 1980, *ApJ (Letters)*, **238**, L27.
- Carlberg, R. G. & Couchman, H. M. P. 1989, *ApJ*, **340**, 47.
- Cioffi, D. F., McKee, C. F., & Bertschinger, E. 1988, *ApJ*, **334**, 252.
- Couchman, H. M. P. & Rees, M. 1988, *MNRAS*, **221**, 53.

- Cox, D. P. & Smith, B. W. 1974, *ApJ (Letters)*, **189**, L105.
- David, L. P., Arnaud, K. A., Forman, W., & Jones, C. 1990, *ApJ*, **356**, 32.
- David, L. P., Forman, W., & Jones, C. 1991, *ApJ*, **369**, 121.
- Davis, M., Summers, F. J. & Schlegel, D. 1992, *Nature*, **359**, 393.
- Dekel, A. & Silk, J. 1986, *ApJ*, **303**, 39.
- Donahue, M. & Shull, M. 1987, *ApJ (Letters)*, **323**, L13.
- Edge, A. C. 1989, Ph.D. Thesis, University of Leicester.
- Efstathiou, G. & Rees, M. J. 1988, *MNRAS*, **230**, 5P.
- Efstathiou, G., Frenk, C. S., White, S. D. M., & Davis, M. 1985, *ApJ*, **57**, 241.
- Efstathiou, G., Frenk, C. S., White, S. D. M., & Davis, M. 1988, *MNRAS*, **235**, 715.
- Feynman, R. P. 1939, *Phys. Rev.*, **56**, 340.
- Gott, J. R. & Rees, M. J. 1975, *Astr. Ap.*, **45**, 365.
- Gunn, J. E. & Peterson, B. A. 1965, *ApJ*, **142**, 1633.
- Hatsukade, I. 1989, Thesis, Osaka University.
- Heckman, T. M., Armus, L., & Miley, G. K. 1990, *ApJ Suppl.*, **74**, 833.
- Holtzman, J. A. 1989, *ApJ Suppl.*, **71**, 1.
- Hughes, J. P., Yamashita, K., Okumura, Y., Tsunemi, H., & Matsuoka, M. 1988, *ApJ*, **327**, 615.
- Ikeuchi, S. & Ostriker, J. P. 1986, *ApJ*, **301**, 522.
- Lea, S. M., Mushotzky, R., & Holt, S. 1982, *ApJ*, **262**, 24..
- McCray, R. & Kafatos, M. 1987, *ApJ*, **317**, 190.
- McCray, R. & Snow, T. P. Jr. 1979, *Ann. Rev. Astr. Ap.*, **17**, 213.
- McKee, C. F. & Ostriker, J. P. 1977, *ApJ*, **218**, 148.
- Miralda-Escude, J. & Ostriker, J. P. 1990, *ApJ*, **350**, 1.
- Mushotzky, R. F. 1984, *Physica Scripta*, **T7**, 157.
- Ostriker, J. P. & Cowie, C. F. 1981, *ApJ (Letters)*, **243**, L115.
- Ostriker, J. P. & McKee, C. F. 1988, *Rev. Mod. Phys.*, **60**, 1.
- Peacock, J. A. & Heavens, A. F. 1990, *MNRAS*, **243**, 133.
- Pettini, M., Boksenberg, A., & Hunstead, R. 1990, *ApJ*, **348**, 48.
- Press, W. H. & Schechter, P. 1974, *ApJ*, **187**, 425.
- Rees, M. J. & Ostriker, J. P. 1977, *MNRAS*, **179**, 541.
- Rees, M. J. 1986, *MNRAS*, **218**, 25P.
- Rothendflug, R. L., Vigroux, R., Mushotzky, R., & Holt, S. 1984, *ApJ*, **279**, 53.
- Schwarz, J., Ostriker, J. P. & Yahil, A. 1975, *ApJ*, **202**, 1.
- Sedov, L. I. 1959; Similarity and Dimensional Methods in Mechanics (Academic, New York).
- Shafi, Q. & Stecker, F. W. 1984, *Phys. Rev. Lett.*, **53**, 1292.
- Shapiro, P. R. 1986, *Pub. A. S. P.*, **98**, 1014.

- Shapiro, P. R. & Giroux, M. 1987, *ApJ (Letters)*, **321**, L107.
- Sherman, R. D. 1980, *ApJ*, **237**, 355.
- Silk, J. I. 1977, *ApJ*, **211**, 638.
- Smoot, G. F. *et al.* 1992, *ApJ (Letters)*, **396**, L1-L18.
- Stebbins, A. & Silk, J. 1986, *ApJ*, **300**, 1.
- Steidel, C. C. & Sargent, W. L. W. 1987, *ApJ (Letters)*, **318**, L11.
- Steidel, C. C. 1990, *ApJ Suppl.*, **74**, 37.
- Terasawa, N. 1992, Preprint
- Tomisaka, K., Habe, H., & Ikeuchi, S. 1980, *Progr. Theor. Phys. (Japan)*, **64**, 1587.
- Weaver, R., McCray, R., Castor, J., Shapiro, P., & Moore, R. 1977, *ApJ*, **218**, 377.
- Webb, J. K., Barcons, X., Carswell, R. F., & Parnell, H. C. 1992, *MNRAS*, **255**, 319.
- White, S. D. M., & Rees, M. J. 1986, *MNRAS*, **183**, 341.

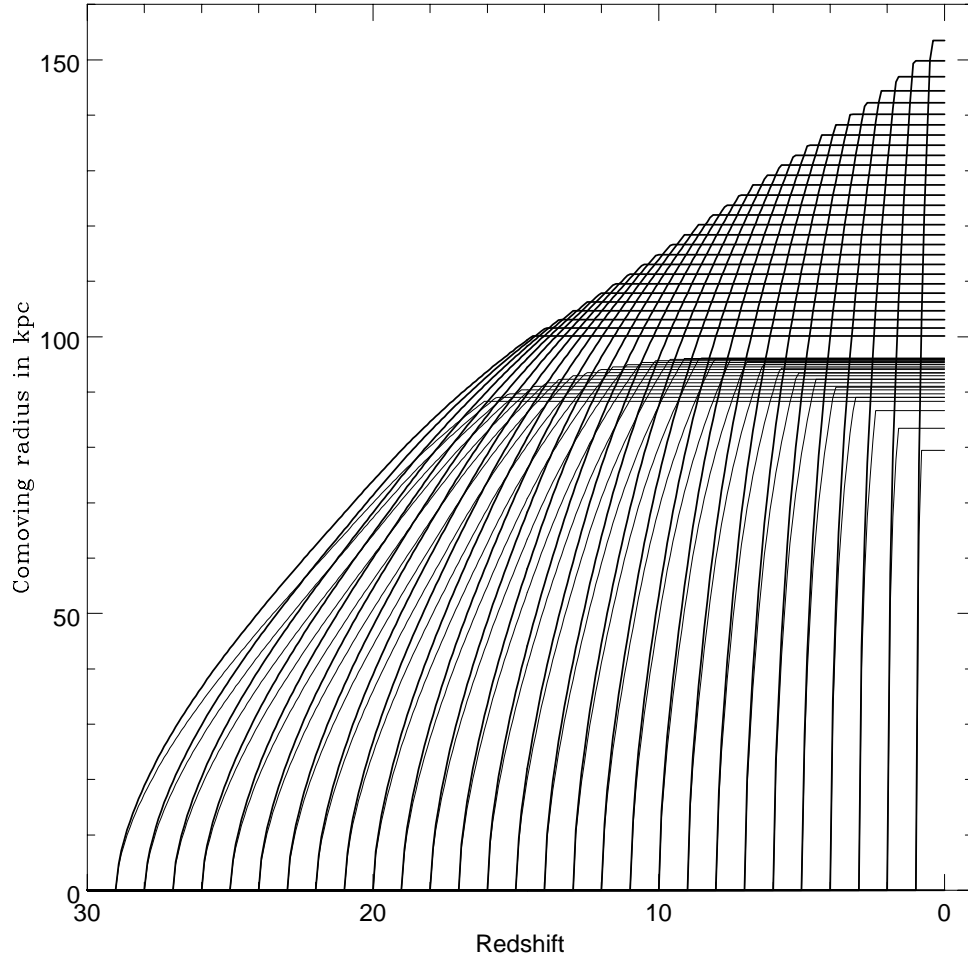


Figure 1: Comoving radius of expanding shell.

The comoving shell radius $(1+z)R$ is plotted for galaxies of total mass $2 \times 10^6 M_\odot$, forming at integer redshifts from 1 to 29. Here $\Omega = 1$, $\Omega_b = 0.06$, $h = 0.5$, and $f_m = 0.1$. $f_d = 1$ for the upper set of lines and $f_d = 0$ for the lower set. R has been truncated when T drops below 15,000 K, after which newly swept up IGM fails to become ionized.

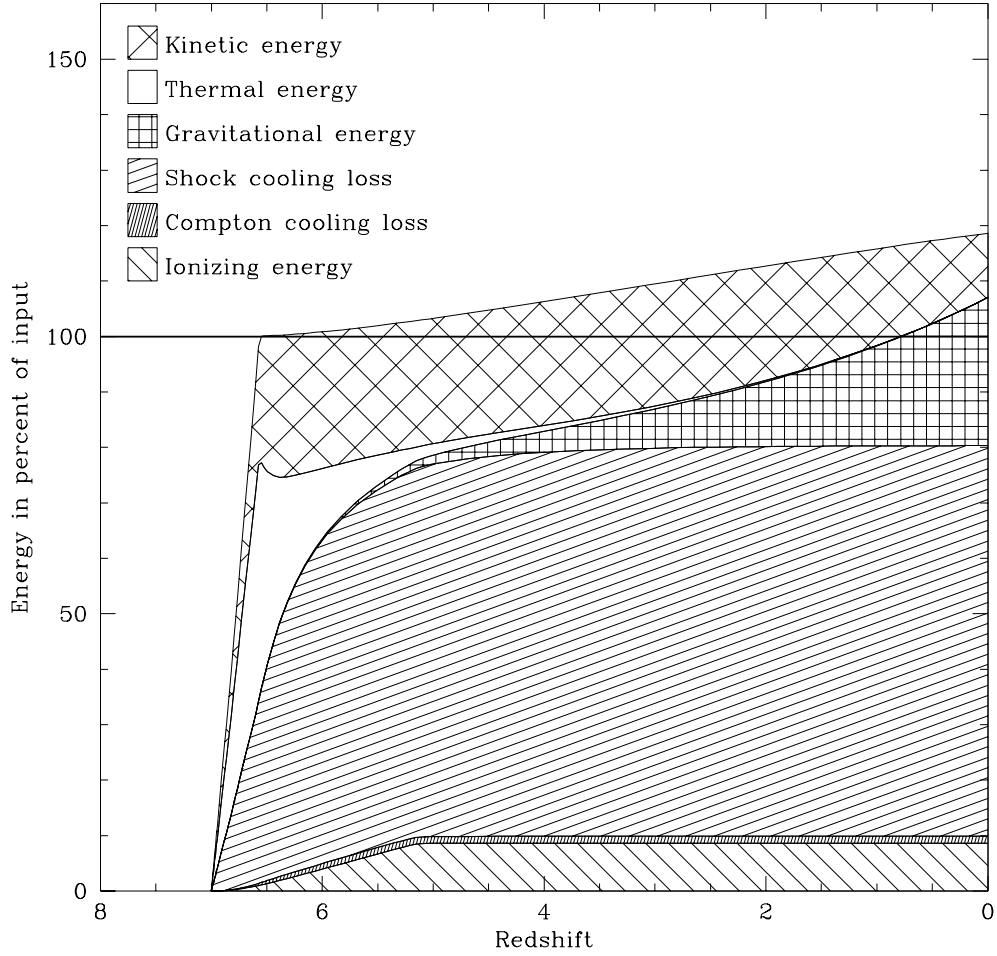


Figure 2: This and the two following figures show the energy contents of an expanding bubble as a function of redshift, for different choices of f_d and z_* . $\Omega = 1$, $\Omega_b = 0.06$, $h = 0.5$ and $f_m = 0.1$ for all three plots. Figures 2 and 3 illustrate the difference between $f_d = 0$ and $f_d = 1$ (there is no shock cooling loss in the second case). Figure 4 has $f_d = 0$ and illustrates that the Compton cooling loss is larger at higher redshift.

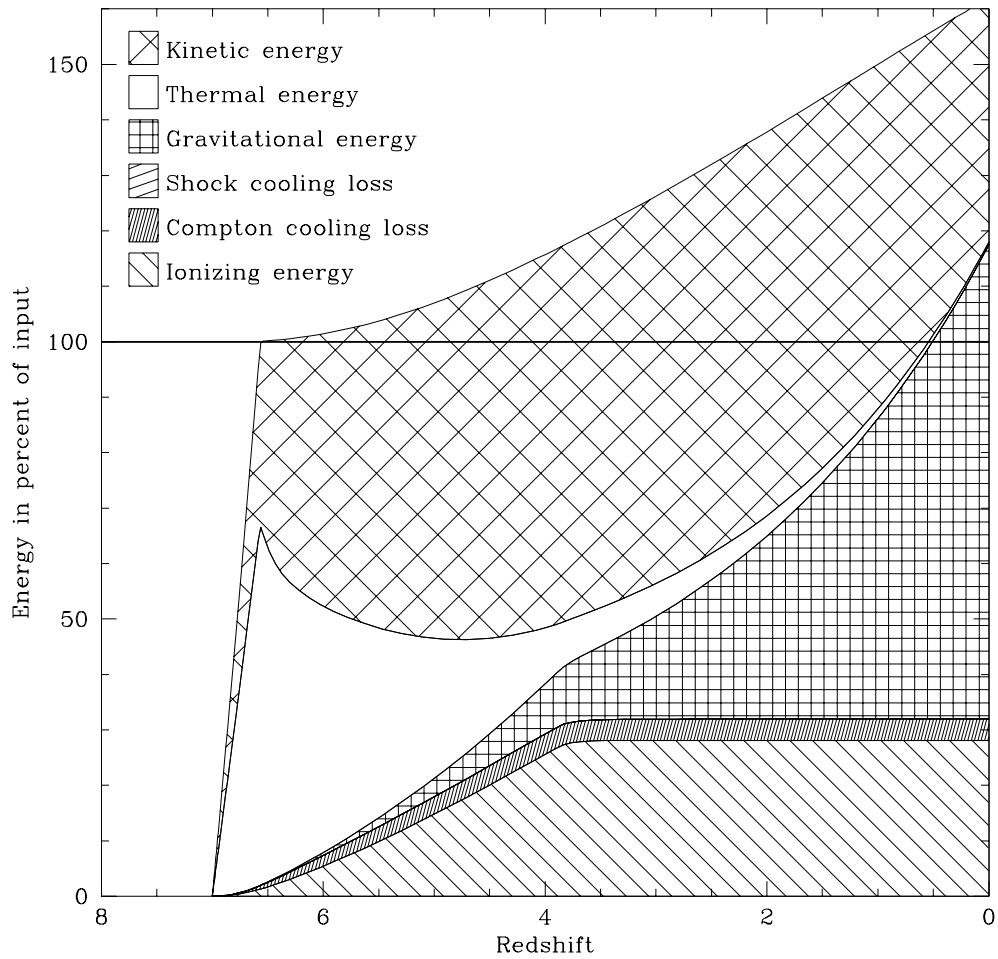


Figure 3: Energetics of expanding shell, example 2.

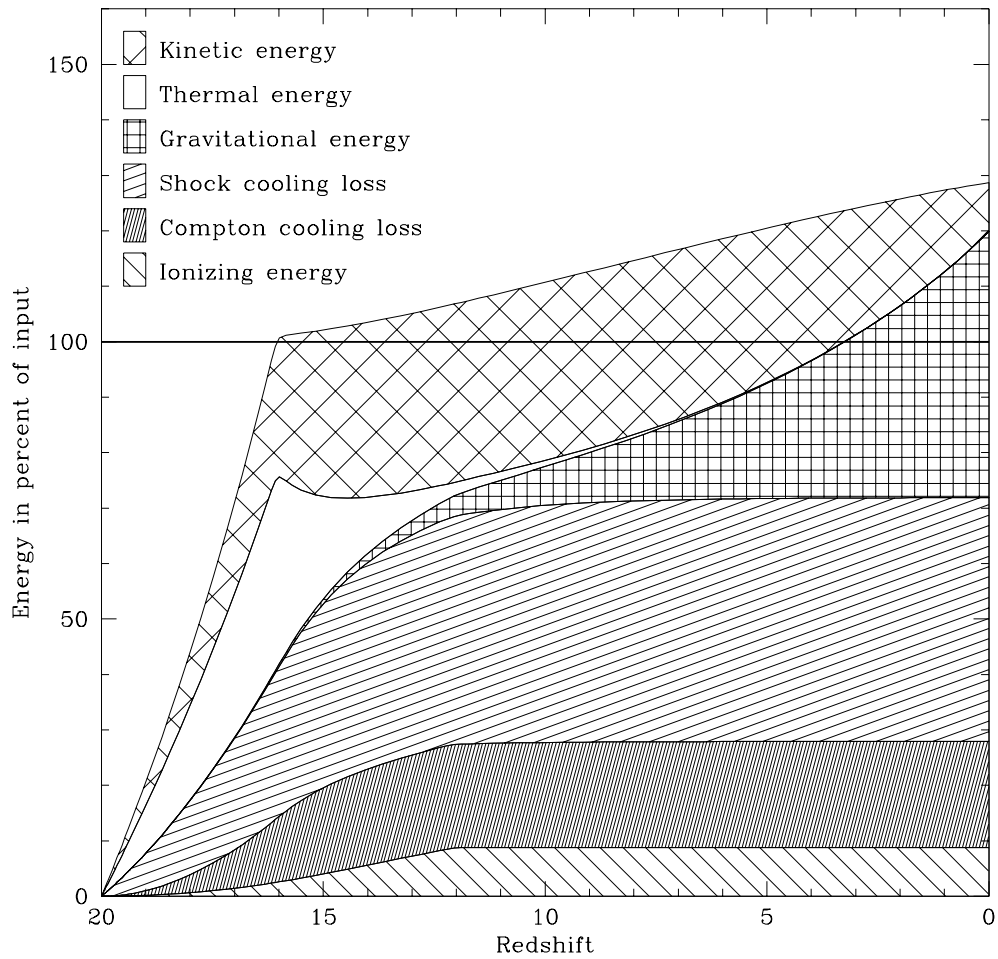


Figure 4: Energetics of expanding shell, example 3.

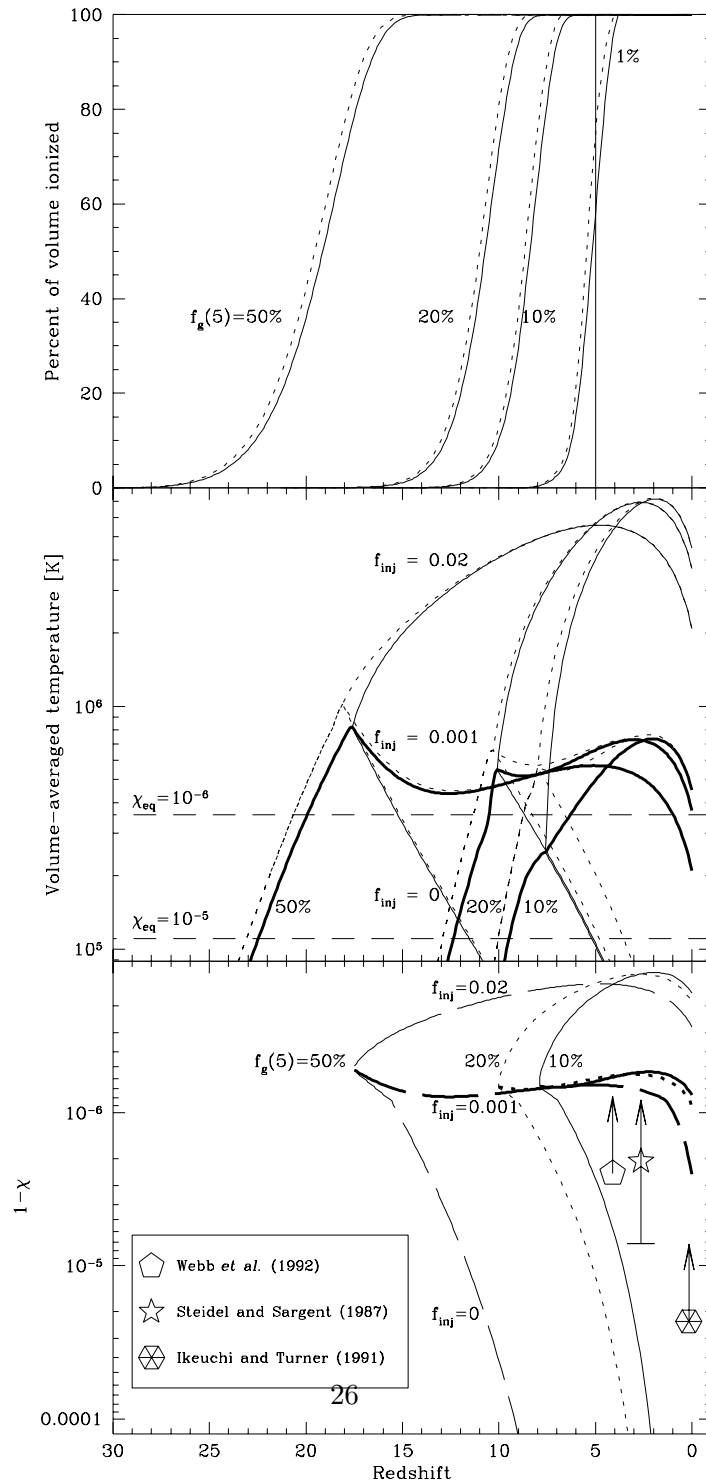


Figure 5: IGM evolution for $M = 2 \times 10^6 M_\odot$

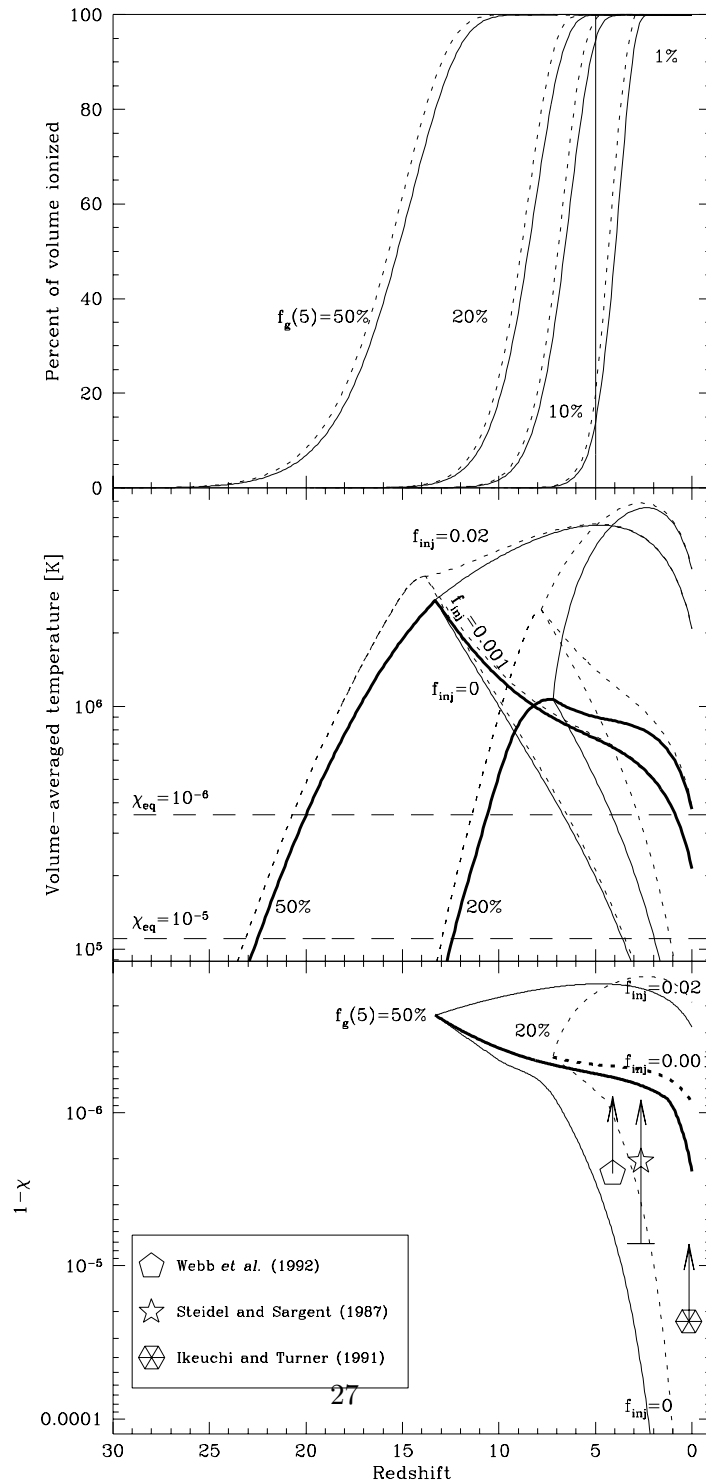


Figure 6: IGM evolution for $M = 10^8 M_\odot$

Figures 5 and 6: IGM evolution.

Three different properties of the IGM (filling factor, temperature and ionization) are plotted as a function of redshift for different choices of M_c , $f_g(5)$ and f_d . $\Omega = 1$, $\Omega_b = 0.06$, $h = 0.5$ and $f_m = 0.1$ in the two previous figures, 5 and 6. In all panels, the different families of curves correspond to different values of $f_g(5)$; 50%, 20%, 10% and 1% from left to right, with the rightmost cases being omitted where they fail dismally. In the porosity and temperature plots (the upper two panels of 5 and 6), dashed lines correspond to $f_d = 1$ and solid ones to $f_d = 0$, whereas only the pessimistic $f_d = 0$ case is plotted in the ionization plots (the lower third). In the temperature and ionization plots (the lower two panels), the three branches of each curve correspond to the three reheating scenarios: $f_{inj} = 0$, $f_{inj} = 0.001$ and $f_{inj} = 0.02$.